13

Influence of ion and acid etching on structural and magnetic resonance characteristics of the epitaxial iron garnet films

© A.A. Syrov, S.V. Tomilin, E.Yu. Semuk, S.V. Osmanov

Vernadsky Crimean Federal University, Simferopol, Russia 295007 Simferopol, Russia e-mail: anatoly199824@rambler.ru

Received October 29, 2024 Revised March 20, 2025 Accepted April 03, 2025

The study presents experimental results of the investigation of the effects of post-growth treatment of the thin single-crystal films of the cation-replaced iron garnets on their structural and magnetic characteristics. It is shown that acid etching of the surface of the single-crystal garnets is usually inferior in the quality of surface treatment to the ion-plasma etching method. During investigating a morphology of the surface layer and spectra of ferromagnetic resonance in the epitaxial iron garnet film, it was shown that using orthophosphoric acid as an etchant resulted in reduction of surface roughness, but did not provide qualitative conservation of the magnetic characteristics as compared to the ion-plasma treatment method, which did not deteriorate the structure and did not destroy a crystal lattice of the iron garnets.

Keywords: ion etching, acid etching, iron garnet, ferromagnetic resonance, edge profile, masking.

DOI: 10.61011/TP.2025.08.61742.374-24

Introduction

With adding rare-earth components, the epitaxial iron garnet films (EIGF) are for quite long time and comparatively successfully widely applied when designing and manufacturing various technical devices. In recent decades, great efforts have been aimed at EIGF application when creating high-sensitivity magnetic field sensors [1-4], including when manufacturing devices and elements based thereon for thermomagnetic information recording [1], mapping of an area and magnetooptical visualization of the inhomogeneous magnetic fields [2,5]. Presently, the sensors of the magnetooptical EIGFs grown on gadolinium-gallium garnet substrates are used for manufacturing various devices in forensic science and medicine [2,6]. The magnetic films based on yttrium-iron garnet are characterized by high magnetic susceptibility and quite low decay values, thereby making it possible to use them in gigahertz band-stop filters, magnetic modulation sensors, phase shifters, directional splitters, magnetic static wave delay lines, for generation of Bose Einstein magnon condensation, etc. [6-15].

An extremely important task of epitaxial material science is to improve efficiency of EIGF use, therefore, one of the directions for solving this problem is surface treatment of the synthesized films [16,17]. It may be necessary both as post-growth treatment (removal of contamination, surface-adsorbed impurities and layers with different properties) as well as for forming a pre-defined profile (reduction of edge stresses, a form factor, etc.) [18–21]. It is also possible to apply a procedure of consecutive off-etching of the epitaxial-film layers for investigating an internal structure of and dimensional dependences of magnetic effects [22]. Accordingly, it is of great interest to study possibilities and influence of the post-growth treatment methods on the

properties of these films. Therefore, during wide studies, it is required to select an optimal surface treatment method to test technological possibilities of manufacturing of the epitaxial films with pre-defined properties.

The surface of the iron garnet films are usually etched by applying methods of chemical treatment (acid, alkali) [23–26] and ion etching (by an ion beam, in a glow and corona discharge) [27–29]. The methods of chemical etching can remove a substance from the film surface at a grater rate, but they are selective in relation to defects and structure nonuniformities. On the contrary, the method of ion etching can ensure EIGF etching at a relatively low rate, which is relevant for the nanometer-thick films, and at the same time they allow implementing anisotropic etching with a high degree of homogeneity along the surface.

The present study is dedicated to investigating influence of the two different methods of post-growth treatment (acid and ion-plasma etching) of the surface of the thin single-crystal films of the cation-replaced iron garnets on their structural and magnetic resonance properties. The provided results demonstrate comparison of effects of the acid and ion-plasma procedures of EIGF surface etching on a state of initial samples based on various tasks of their application.

1. Experimental procedures

The present study applies the liquid-phase epitaxy method for synthesis of the single-crystal EIGF samples, which consists of crystallization of the films from a supersaturated solution-melt. In order to create a pre-defined solution-melt, a blend of garnet-generating components, a low-melting solvent and additional matching additives is melt in a special crucible at the temperatures of about 1390 K for 3–4 h with

subsequent homogenization at this temperature for $9-10\,h$. Of which, from 2 to $4\,h$ — with permanent mixing by a platinum mixer, then the temperature of the solution-melt is gradually reduced to the temperatures below a saturation point (about $1210-1240\,K$) for $2\,h$.

Nonmagnetic single-crystal garnets are used as substrates. The substrate is immersed into the solution-melt and serves as a seed for growth of the epitaxial film, while the temperature of the system is kept constant. With qualitative selection of dopants and growth modes, it is possible to achieve minimum mismatch of the lattice parameters of the single-crystal substrate and the synthesized film Δa , thereby allowing forming the epitaxial layers with higher structural perfection and a pre-defined direction of crystallographic anisotropy.

The research object is EIGF films grown on the single-crystal substrates of the gadolinium-gallium garnet $Gd_3Ga_5O_{12}$ (GGG), of the thickness of $500\,\mu\mathrm{m}$ with the (111) surface orientation. The single-crystal films of the iron garnet of the composition (YLa)₃(FeGaAl)₅O₁₂ (of the thickness of $2.1\,\mu\mathrm{m}$) were produced using the technology of crystallization from the supersaturated solution-melt, which contains garnet-generating elements, dopants and matching elements in the low-melting solvent PbO-Ba₂O₃ [30].

The ion-plasma and/or acid treatment of the EIGF surface is used as post-growth treatment to remove surface layers of the synthesized films as well as to form the structure with a certain planar configuration and a spatial profile (for example, when recording the ferro-magnetic resonance (FMR) spectra for reducing additional signals related to excitation of the magnetic static waves and presence of edge defects).

The ion-plasma treatment of the synthesized singlecrystal samples was carried out by ions of HF-plasma obtained in a mixture of the gases Ar (60 mol%) + + O₂ (40 mol%) at the pressure of 1 Pa using a small-scale vacuum installation of deep anisotropic etching "MVU TM Plazma 06" (NIITM, Zelenograd). The material was etched as a result of physical interaction between the argon ions accelerating in the plasma and the atoms of the surface layer film in the low-pressure conditions. At the same time, it is possible to disturb oxygen stoichiometry in sub-surface layers of the iron garnet film. This negative effect on the film structure is exactly partially compensated by adding oxygen into a reaction volume (an optimal concentration is determined empirically). At the same time, the etching rate is reduced, but the surface quality improves and, consequently, the influence of the surface defects on the film properties is reduced. Use of the oxygen plasma for anisotropic etching of the iron garnet films with improvement of surface roughness is also described in the study [22]. The planar structures with a pre-defined etching profile were created in this study by using a nonmagnetic solid-state mask of plane-parallel GGG plates [31].

Acid treatment was presented by a classic technology of etching in orthophosphoric acid H₃PO₄ at the temperature of 200 °C with application of a planar mask based on

the photoresist of the grade FP-383 for forming the round profile. The photoresist layer was applied by a method of fast centrifugation to a pre-prepared surface by a uniform layer of the thickness of up to $3\,\mu\mathrm{m}$ with subsequent exposure through a photo pattern. More details about the mask creation technology and the procedure of acid etching can be found in the papers [32–34].

A height of the off-etched layer in an investigation point of the sample h(x) was measured using the Linnik micro-interferometer MII-4 with a digital processing unit. The height was determined by a value of the shift of the interference pattern according to the formula

$$h(x) = \frac{a(x)}{2b} \lambda,$$

where a(x) — the value of the shift of the interference pattern in the studied point x; b — the value of the interference period, λ — the wavelength of radiation (a green light filter with $\lambda = 532 \, \mathrm{nm}$ was applied in the present study).

The magnetic resonance properties of the epitaxial films (generation of basic and MSW modes, presence of structurally-related noises, etc.) were studied by analyzing ferro-magnetic resonance (FMR) spectra obtained in the SPINSCAN X spectrometer. The spectrometer is designed to study differential FMR spectra in field scanning in two configurations of orientation of the external magnetic field in relation to a plane of the studied film: perpendicular (0° in relation to the normal) and parallel (90°).

The surface morphology was studied by atomic-force microscopy in the Ntegra equipment produced by NT-MDT. By detecting a force of interaction between a probe and the surface of the studied EIGF sample during gradual transmission of the probe above the entire pre-defined area of the film, it is possible to study surface irregularities.

2. Results and discussion

2.1. Formation of the profile when etching through the mask

The thin-film structures with the pre-defined geometry were produced by using etching of the film surface with application of a mask, wherein the mask-covered surface was not etched. The method of acid and ion-plasma etching of the epitaxial iron garnet film of the composition $(YLa)_3(FeGaAl)_5O_{12}$ and of the thickness of $h=2.1\,\mu\mathrm{m}$ was taken to manufacture discs of the diameter of 2 and 3 mm. Fig. 1 shows the cross-sectional profiles of the formed discs. The profiles were obtained with radial scanning by means of the Mitutoyo SJ-410 profilometer.

It is clear that during ion-plasma treatment of the EIGF surface a boundary of the dielectric mask originates edge effects that are related to formation of an induced static charge [21] and result in formation of a nonuniformity of the ion flux and "compaction" of the plasma in an area adjacent to the mask edge. It results in etched depressions

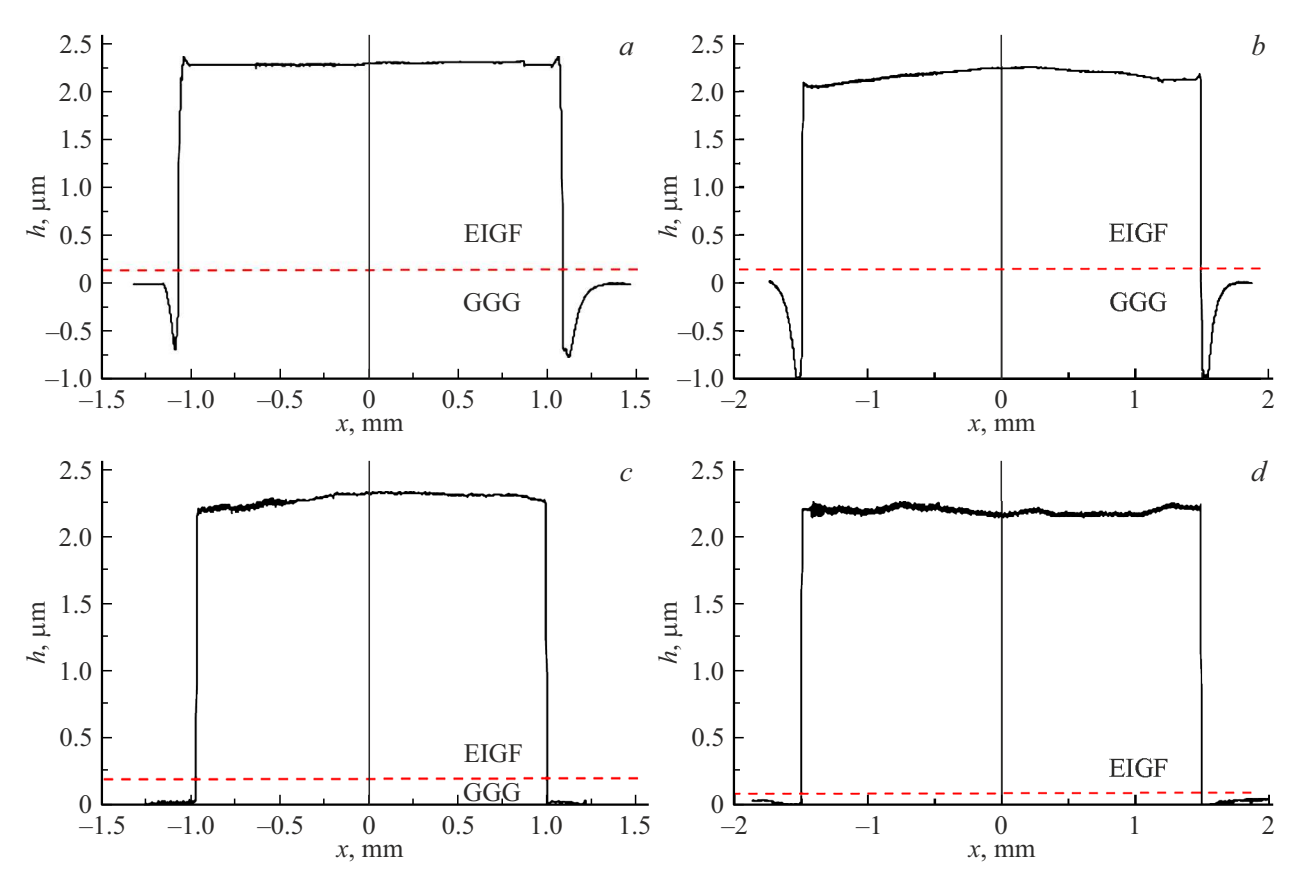


Figure 1. Cross-sectional profile of the discs produced by the methods of ion-plasma etching (a, b) and acid etching (c, d), the discs of the diameter of 2 mm (a, c) and the diameter of 3 mm (b, d). The dashed line shows a boundary between the EIGF film and the GGG substrate.

in the substrate along a perimeter of the masked part of the film (Fig. 1, a, b). But these artefacts do not affect a structure of the side surfaces of the formed disc structure.

With acid etching, the described edge effects are less pronounced (Fig. 1, c, d), thereby making it possible to form a clearly pronounced step at the zone edge without significant distortions of a rectangular profile.

Thus, both the methods ensure formation of quite clear profiles of the masked EIGF area with minimum distortion of the side facets of the structure at the etching boundary. The influence of this profile on the magnetic resonance properties of the structures will be shown below.

2.2. Surface structure in layer-by-layer etching

Since the surface quality and the structural EIGF perfection, including that is formed during post-growth treatment, significantly affects efficiency of their practical application, the influence of acid and ion etching on the structure of the film surface was studied. The EIGF morphology (YLa)₃(FeGaAl)₅O₁₂ (the square 5×5 mm of the thickness of $h=2.1\,\mu\text{m}$) was analyzed by means of AFM scanning in layer-by-layer etching of the surface. The obtained results were compared by several parameters, namely, a maximum height spread A_{max} and a root mean square of deviation from the average value (in essence, average roughness).

The initial sample of the magnetic film has the maximum height spread A_{max} is 51.2 nm, while the root mean square deviation RMS = 1.4 nm.

After ion off-etching of the upper layer of the thickness of $0.5 \,\mu\mathrm{m}$ (the residual thickness of the film is $1.6 \,\mu\mathrm{m}$), more than two-times reduction of the value of the spread parameter can be observed (Fig. 2, a); thus, the value of A_{max} was 18.9 nm, while the root means square deviation RMS was 1.2 nm. After the second stage of etching (Fig. 2, b), with total removal of the layer of the thickness of $1 \mu m$ (the residual thickness is $1.1 \mu m$) the values of the parameters are reduced to be $A_{\text{max}} = 7.3 \,\text{nm}$ and RMS = 0.8 nm, respectively. As a result of the third cycle of ion treatment (Fig. 2, c), with total off-etching of the layer of the thickness of 1.5 μ m (the residual thickness is 0.6 μ m) there is still a general trend of reduction of the values of the studied parameters. In this case the value of A_{max} is already 6.7 nm, while the root mean square RMS is 0.5 nm.

The influence of acid etching on the parameters of morphology of the EIGF surface were similarly studied (Fig. 3).

It is clear that after the first stage of acid etching (Fig. 3, a) as a result of removal of the layer of the thickness of $0.5\,\mu m$ (the residual thickness of the film is $1.6\,\mu m$) the root mean square deviation RMS is $1.1\,nm$, while the maximum height spread is $A_{max}-34.1\,nm$. After total removal of the

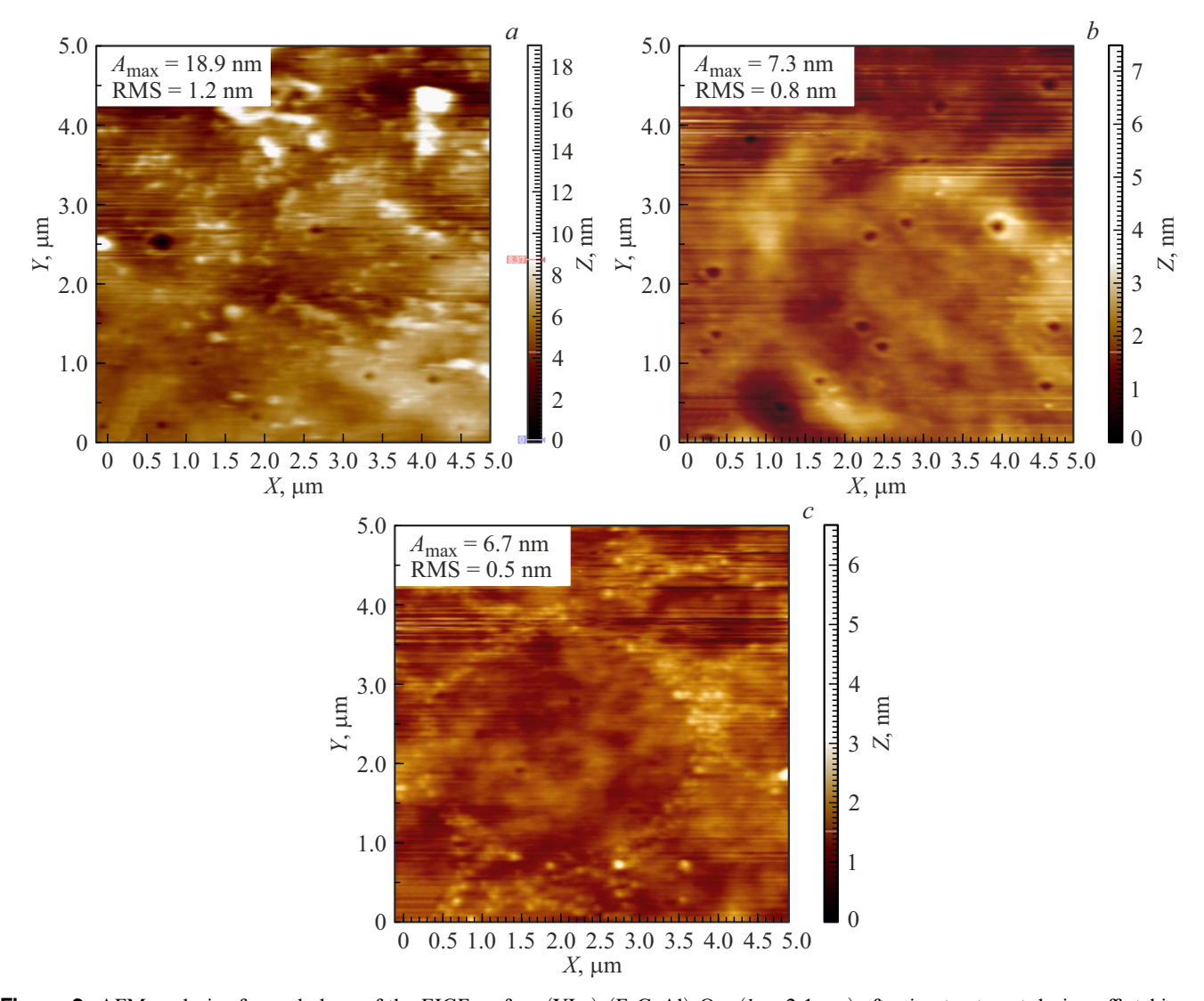


Figure 2. AFM analysis of morphology of the EIGF surface $(YLa)_3(FeGaAl)_5O_{12}$ $(h = 2.1 \,\mu\text{m})$ after ion treatment during off-etching of the layer of the thickness of 0.5 (a), 1 (b) and 1.5 μ m (c).

layer of the thickness of $1 \mu m$, with the residual thickness of $1.1 \,\mu m$ (Fig. 3, b), the room mean square deviation RMS is almost unchanged to be 1.2 nm, whereas the maximum height spread of the relief is reduced to 14.1 nm. the final third stage of etching (Fig. 3, c) with removal of $1.5 \,\mu\text{m}$ (the residual thickness is $0.6 \,\mu\text{m}$) the values of the said parameters are reduced to be $A_{\text{max}} = 7.3 \text{ nm}$, RMS = 0.7 nm.

Fig. 4 shows variation of the roughness parameters of the EIGF surface in layer-by-layer etching by the different methods. The abscissa axis is taken to show the thickness of the removed layer (an etching depth).

Thus, it is clear that in layer-by-layer ion etching of the epitaxial film there is significant reduction of the values of the root mean square deviation and the maximum roughness height spread. In the observed experiments, the method of ion etching provides an average smaller value of the roughness parameters as compared to the method of acid etching.

Specific features of FMR in layer-by-layer etching

In order to analyze the influence of ion etching on the magnetic properties of the EIGF, the specific features of FMR were studied for all the above-described structures with a different configuration of the external bias field. Fig. 5 shows FMR spectra when the external field is parallel to a normal to the film (perpendicular resonance). Fig. 5, a shows the FMR spectrum of the initial iron garnet film shaped as a square with a side of 5 mm. The spectrum can have a group of lines distinguished within the range 406-418 mT, which corresponds to a volume mode with the main resonance line of 415 mT modulated by resonances of magnetic static waves (MSW) as well as a separate resonance line at 426 mT, which is related to a surface mode.

When the sample geometry is changed by a circle of the radius of $1.5 \,\mathrm{mm}$ (Fig. 5, b), the FMR spectrum exhibits changes related to efficiency of MSW excitation

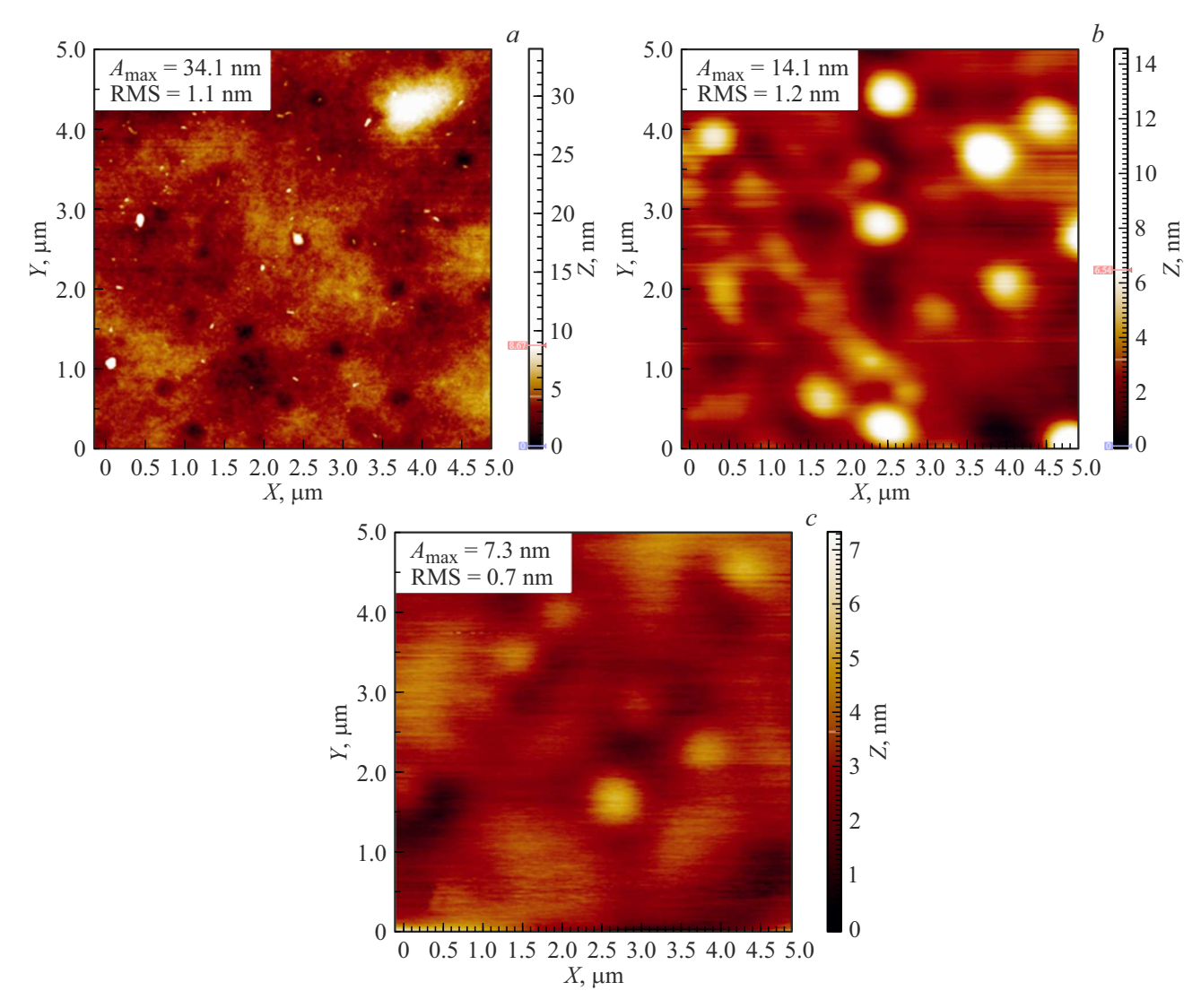


Figure 3. AFM analysis of morphology of the EIGF surface $(YLa)_3(FeGaAl)_5O_{12}$ $(h=2.1\,\mu\text{m})$ after acid treatment during off-etching of the layer of the thickness of 0.5 (a), 1 (b) and 1.5 μ m (c).

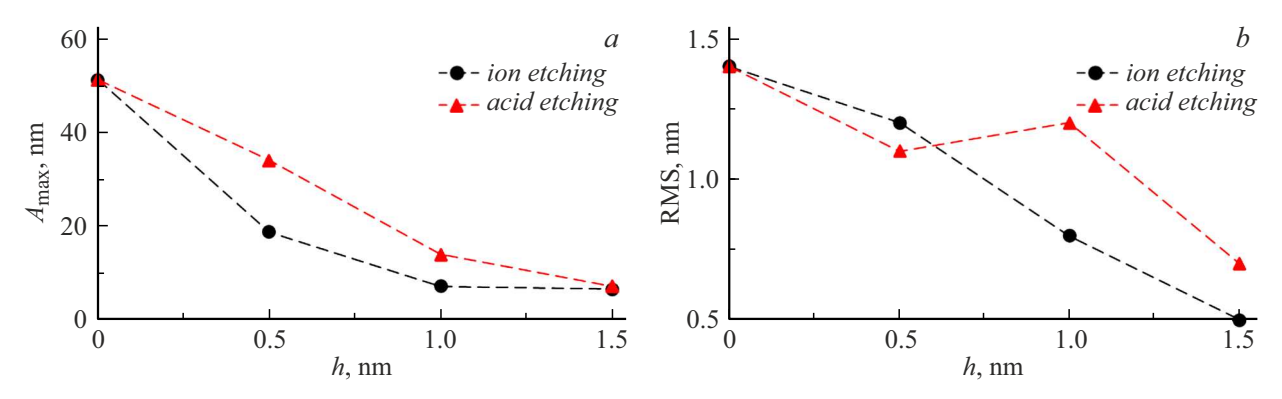


Figure 4. Variation of the roughness parameters of the EIGF surface in layer-by-layer etching by the different methods; a — the parameter A_{max} , b — the parameter RMS.

as compared to the basic mode, while a position of the spectrum lines is not changed. The similar changes are observed when the circle radius is reduced to 1 mm

(Fig. 5, c). At the same time, the basic line at 415 mT is clearly pronounced against the background of relatively weak MSW signals. It should be noted that since there

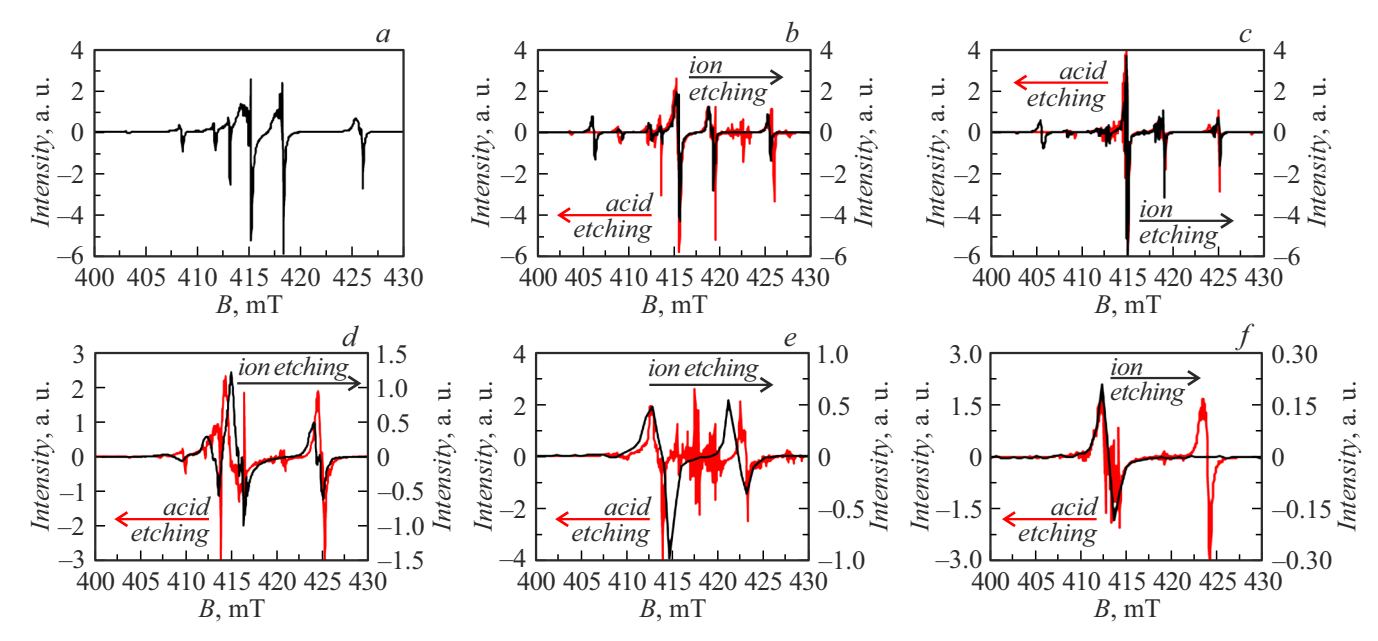


Figure 5. Resonance curves of FMR (the film $(YLa)_3(FeGaAl)_5O_{12}$, $h=2.1\,\mu\text{m}$) for perpendicular (0°) resonance (the red line — acid etching, the black line — ion etching); a — the square $(h=2.1\,\mu\text{m})$, before treatment), b — the disc $R=1.5\,\text{mm}$, c — the square $(h=1.6\,\mu\text{m})$, e — the square $(h=1.1\,\mu\text{m})$, f — the square $(h=0.6\,\mu\text{m})$.

is no effect on the surface of the masked area (only the film outside the mask is removed), a mode of surface oscillations does not change when the planar form of the sample is changed. Similarly, the form of the spectrum is insignificantly affected by the etching method as well, because, as shown above (Fig. 1), the shape of the profile of the produced disc is almost the same for both the methods.

FMR is slightly different in layer-by-layer removal of a film portion without changing the planar form. It is clear from Fig. 5, d that removal of a layer of the thickness of 500 nm (about 1/4 of the film thickness) on the surface of the initial EIGF shaped as a square a spectrum of MSW modulation of the volume mode is less pronounced, while the lines themselves are in a lesser number and they are arranged further away. The mode of surface oscillations is more pronounced as well. It should be noted that the FMR spectrum of the sample produced in ion etching exhibits less noise pollution by the MSW modes as compared to acid etching, which is caused by better roughness parameters of the surface. After ion off-etching of the layer of the thickness of $1 \mu m$ (Fig. 5, e) the FMR spectrum of the sample has only two homogeneous lines of the volume and surface modes. The FMR spectrum of the sample after acid etching also has the two modes of volume and surface oscillations, and at the same time it includes stronger noise pollution by the MSW modes. Ion off-etching of the layer of the thickness of $1.5 \,\mu\mathrm{m}$ (Fig. 5, f) results in formation of the FMR spectrum with one clearly pronounced resonance mode. After acid etching the FMR spectrum still has the two modes, while the number of additional MSW resonances is reduced, which can be related to reduction of surface roughness (Fig. 4).

Similar dynamics of variation of the FMR spectra is also observed in the parallel configuration, when the external field vector is in a plane of the film (Fig. 6). Thus, when the planar form of the sample is changed (Fig. 6, a-c), a set of the MSW modulating lines is the same and only intensity of the MSW lines in relation to the basic line of the FMR volume mode is changed. In this case, the form of the spectra likewise weakly depends on the etching method used.

Since we are dealing with the film that has a "light plane" type of magnetic anisotropy (the resonance fields in the parallel configuration are smaller than in the perpendicular one), there is no surface mode in this configuration.

When the thickness of the iron garnet film is changed without change of the planar structure (Fig. 6, a, d–f), there is also observed reduction of the number of the MSW modulating lines as the film thins. At the same time, for the samples produced by the method of acid etching, the FMR spectra for the parallel configuration of the field exhibit high noise pollution by the MSW signals similar to the FMR spectra in the perpendicular configuration.

Tables 1,2 show results of evaluation of the magnetic resonance characteristics of the films (the resonance fields B_{res} , the width of the resonance lines ΔB , the gyromagnetic ratio γ and the effective anisotropy field H_{eff}), which are obtained from analysis of the FMR spectra after ion and acid etching, respectively. The data are provided both for the basic resonance mode (BM) and the surface mode (SM) for the following samples of the film (YLa)₃(FeGaAl)₅O₁₂:

- 1. EIGF square, $h = 2.1 \mu \text{m}$ (before treatment) (Fig. 5, a, 6, a);
 - 2. EIGF disc $R = 1.5 \,\text{mm}$ (Fig. 5, b, 6, b);
 - 3. EIGF disc R = 1 mm (Fig. 5, c, 6, c);

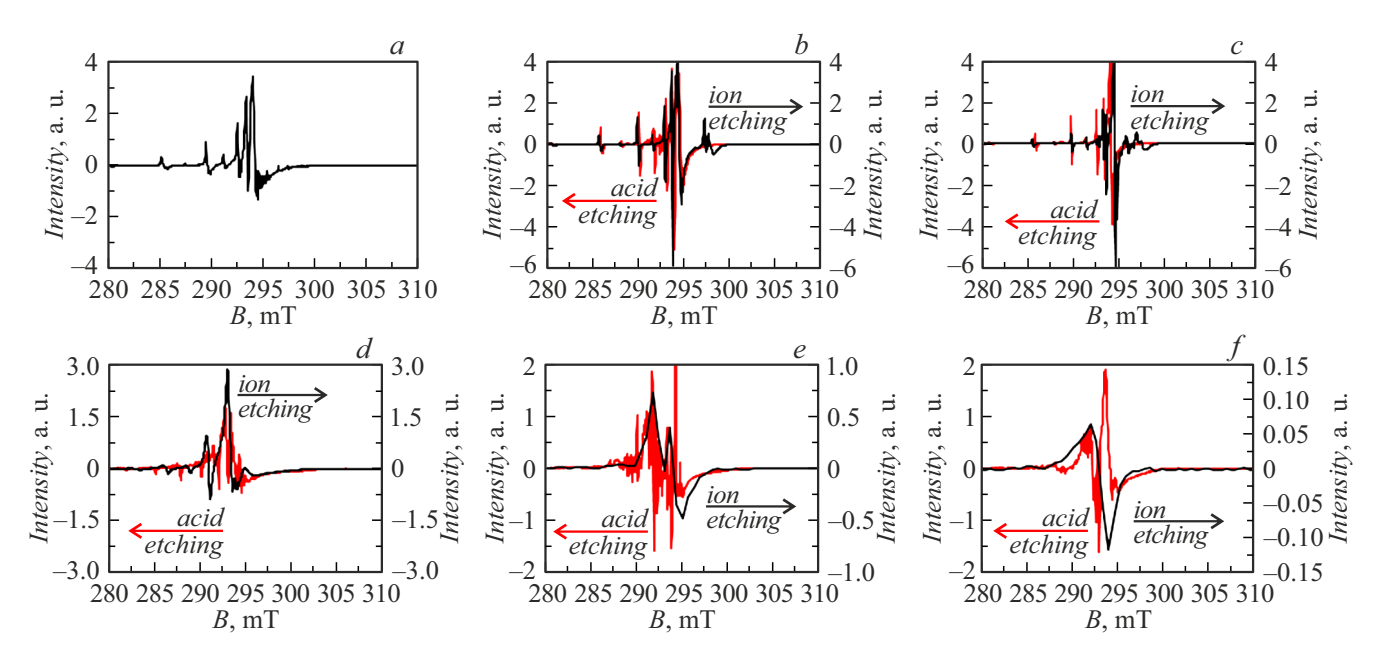


Figure 6. Resonance curves of FMR (the film $(YLa)_3(FeGaAl)_5O_{12}$, $h=2.1\,\mu\text{m}$) for parallel (90°) resonance (the red line — acid etching, the black line — ion etching); a — the square $(h=2.1\,\mu\text{m})$, before treatment), b — the disc $R=1.5\,\text{mm}$, c — the disc $R=1\,\text{mm}$, d — the square $(h=1.6\,\mu\text{m})$, e — the square $(h=1.1\,\mu\text{m})$, f — the square $(h=0.6\,\mu\text{m})$.

	B_{res} , mT			ΔB , mT			$\gamma \cdot 10^{-7}, \mathrm{s}^{-1} \cdot \mathrm{E}^{-1}$		H_{eff} , E	
$N_{\overline{0}}$	0°		90°	0°		90°	γ·10 , δ ·Ε		Heff, E	
	BM	SM	BM	BM	SM	BM	BM	SM	BM	SM
1	415.2	426.1	294.3	1.2	0.9	0.5	1.773	1.756	-822.9	-898.6
2	414.8	424.9	294.2	0.9	0.3	0.5	1.774	1.758	-820.8	-890.9
3	414.4	424.3	294.5	0.6	0.4	0.7	1.774	1.758	-815.9	-884.7
4	415.1	423.7	293.3	1.6	0.8	1.4	1.777	1.763	-829.2	-888.9
5	414.1	422.5	294.4	2.1	1.6	3.1	1.775	1.761	-814.6	-872.9
6	412.6	_	294.3	1.5	_	1.9	1.777	_	-804.9	_

Table 1. Magnetic resonance parameters of the EIGF after ion etching

Table 2. Magnetic resonance parameters of the EIGF after acid etching

	B_{res} , mT			ΔB, mT			$\gamma \cdot 10^{-7}, \mathrm{s}^{-1} \cdot \mathrm{E}^{-1}$		H_{eff} , E	
$N_{\overline{0}}$	0°		90°	0°		90°	y 10 , s 1L		Heff, L	
	BM	SM	BM	BM	SM	BM	BM	SM	BM	SM
1	415.2	426.1	294.3	1.2	0.9	0.5	1.773	1.756	-822.9	-898.6
2	415.3	425.4	294.1	1.0	0.4	0.6	1.774	1.757	-825.0	-895.1
3	413.8	424.2	294.7	0.8	0.5	0.9	1.774	1.757	-810.4	-882.6
4	414.8	424.8	293.7	2.0	0.9	3.0	1.776	1.760	-824.3	-893.8
5	413.4	423.1	293.4	1.6	0.9	4.6	1.780	1.764	-817.6	-884.0
6	412.9	424.0	294.2	2.1	1.0	2.2	1.777	1.759	-807.6	-884.7

^{4.} EIGF square, $h = 1.6 \,\mu\text{m}$ (Fig. 5, d, 6, d);

The said parameters were correctly analyzed, especially when determining the width of the resonance line, by using plotting of the integral FMR spectra (Fig. 7) based on the measured differential spectra (Figures 5 and 6). It is necessary due to presence of a large amount of noises at the differential FMR spectra, which are caused by modulation of the basic resonance lines.

^{5.} EIGF square, $h = 1.1 \,\mu\text{m}$ (Fig. 5, e, 6, e);

^{6.} EIGF square, $h = 0.6 \,\mu\text{m}$ (Fig. 5, f, 6, f).

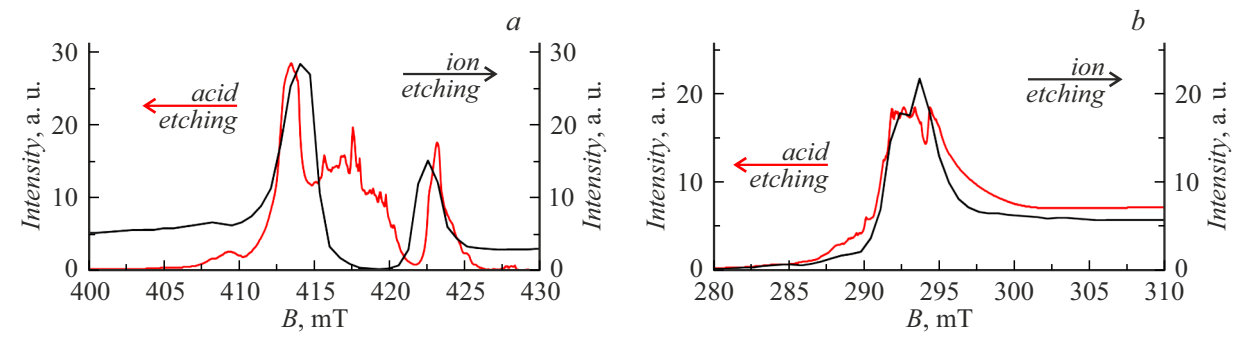


Figure 7. Exemplified plotting of the integral FMR spectra based on the differential spectra (Fig. 5, 6) for the EIGF film of the thickness of $h = 1.1 \, \mu \text{m}$; a— the perpendicular resonance (0°), b— the parallel resonance (90°).

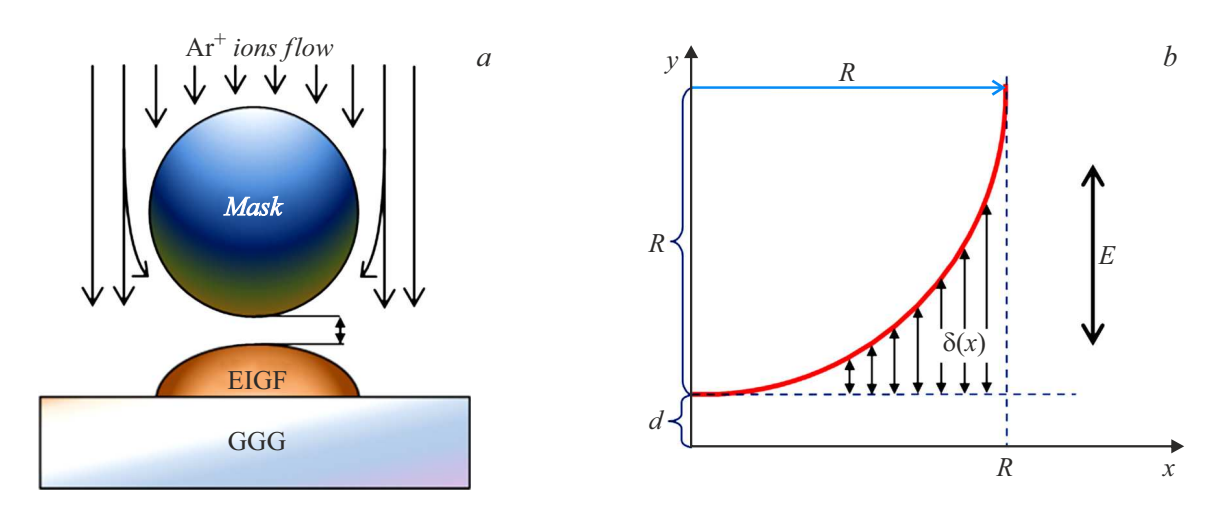


Figure 8. Ion-plasma etching using the spherical mask: the etching scheme (a), the considered model (b).

As it is clear from the presented results, the different methods of etching of the EIGF surface provide similar numerical values of the main magnetic resonance parameters. But it is still worth noting significant noise pollution of the FMR spectra for the films after acid etching.

2.4. Influence of the spatial form of the film on the magnetic properties

The thin magnetic films based on iron-yttrium iron garnet that is applied for solving practical tasks when measuring ultra-weak magnetic field [35] are required to have small values of decay and significant magnetic susceptibility. In this case they can be used as sensitive elements in the magnetic modulation sensors [32,36]. The main limiting factor of qualitative dynamic remagnetization of the magnetic modulation sensors is origination of interference due to origination of edge magnetic domains around boundaries of the film sample. Interaction of the edge domains with the film defects during remagnetization results in formation of additional noises. In order to reduce the influence of the edge domains, the spatial profile of the sensitive element of the sensor, which is shaped as a film disc, shall be preferably formed as smooth as possible tending to an

ellipsoid one in the limit [3]. In order to solve the present problem, we have developed a technology for creating the near-elliptic smooth profile by arranging shaped masks of the nonmagnetic dielectric on the surface of the magnetic film

2.4.1. Principle of formation of the elliptic profile in ion etching

In particular, the elliptic profile of etching is obtained by applying the spherical mask (Fig. 8, a) raised above the film surface at the fixed distance d. Thus, a thickness-heterogeneous gap is formed between the mask and the film surface. Since high-frequency etching is applied for etching of the dielectrics, in various portions of the sample the argon ions being accelerated in the field pass over the different distances $S = \delta + d$ (Fig. 8, b) in the gap between the working surface and the mask, where δ is a path length of the ion with the zero gap between the film and the mask. Thus, the ions acquire a different kinetic energy Q, which will be determined by the distance S (the free path length). The model built on this principle suggests evaluation of efficiency of surface dissipation by the accelerated ions in the variable electromagnetic field, when they move in the

gap between the flat EIGF surface and the spherical surface of the solid mask.

The distance S travelled by the Ar^+ ion under effect of accelerating voltage:

$$S = d + \delta = s + R\left(1 - \sqrt{\frac{x^2}{R^2}}\right),$$

where R is a radius of the spherical mask arranged above the surface of the epitaxial film.

The equation of motion of an electron under effect of the variable electric field:

$$\frac{d^2y}{d\tau^2} = \frac{q}{m} E_0 \sin(\omega \tau),$$

it is solved to obtain a dependence of the distance travelled by the electron in the field on time:

$$S = y = \frac{qE_0}{m} \int d\tau \int \sin(\omega\tau) d\tau$$
$$= \frac{qE_0}{m\omega^2} (-\sin(\omega\tau)) + \text{const.}$$
(1)

Taking into account the boundary conditions, the expression (1) will take the following form

if
$$\tau = 0$$
 $S = 0 \rightarrow \text{const} = 0$,
$$S = C_0 \sin(\omega \tau), \tag{2}$$

where

$$C_0 = -\frac{qE_0}{m\omega^2}.$$

By expressing τ from (2) and substituting into the expression for field strength, we obtain

$$E = E_0 \sin(\omega \tau) = E_0 \frac{S}{C_0} = CS, \tag{3}$$

where $C = E_0/C_0$.

Taking into account (3), the accelerating voltage is:

$$dU = E(S)dS = CSdS$$
,

$$U = C \int SdS = \frac{C}{2} S^2 + \text{const.}$$

We introduce the boundary conditions

if
$$S = 0$$
 $U = 0 \rightarrow const = 0$.

Then, the expression for the accelerating voltage will take the following form

$$U = \frac{C}{S}S^2.$$

Thus, the energy of the argon ions, depending on the distance S travelled by them in the gap between the spherical mask and the treated surface will be described by the quadratic function

$$Q = Uq = \frac{Cq}{2} S^2.$$

At the same time, probability of surface dissipation will be proportional to

$$P \sim \exp\left(\frac{Q}{W}\right),$$

where W is an energy of yield (knocking-out) of the atom from the surface.

Then, the rate of dissipation of the surface by the accelerated argon ions in various points of the surface v(x) can be described by the Arrhenius equation (probability of activation):

$$v = v_{Q \gg W} \exp\left(-\frac{2W}{qCS^2}\right),$$

where $v_{Q\gg W}$ is the value of the rate of dissipation provided that $O\gg W$.

Thus, availability of the heterogeneous slit gap between the film surface and the spherical mask's surface result in a space-heterogeneous field of the etching rates and formation of the near-elliptic profile.

2.4.2. Formation of the elliptic profile of the iron garnet film

The technology of creation of the film elements with the elliptic profile is shown in Fig. 9. It takes several phases to first form the disc 2 from the EIGF I and then the elliptic profile 3 (Fig. 9). The phase $1 \rightarrow 2$ suggests that the surface of the EIGF sample shaped as a square of the size 5×5 mm is covered by a mask produced as a plate of the thickness of 0.5 mm from the single-crystal garnet $Gd_3Ga_5O_{12}$ shaped as a disc of the diameter of 3 mm and then the first stage of ion etching is carried out for a depth that is equal to the EIGF thickness. The respective transverse profile of the disc after etching of EIGF $(YLa)_3(FeGaAI)_5O_{12}$ of the thickness of 2μ m is shown in Fig. 10, a, while the dash-and-dot line marks the boundary of an interface of the EIGF film and the GGG substrate.

During the phase $2 \rightarrow 3$, a spherical ceramic mask of the diameter of 3 mm is arranged on the surface of the created disc structure and the second state of ion etching is carried out. The etching results (Fig. 10, b) in the smooth profile of the height of $2\,\mu{\rm m}$ and the width of 3 mm, which is shaped as a near-elliptic profile. The dash-and-dot line marks the boundary of the interface of the film and the substrate and the dashed line marks the model approximation of the profile. The etching profile obtained by means of a probe profilometer demonstrates good compliance between the model and the experimental results.

2.4.3. FMR in the films with the different profile

The influence of the spatial form of the film was analyzed by studying the specific features of FM with the parallel (90°) and the perpendicular (0°) direction of the bias field B in relation to the film plane. The results of the study after each phase of ion treatment are shown in

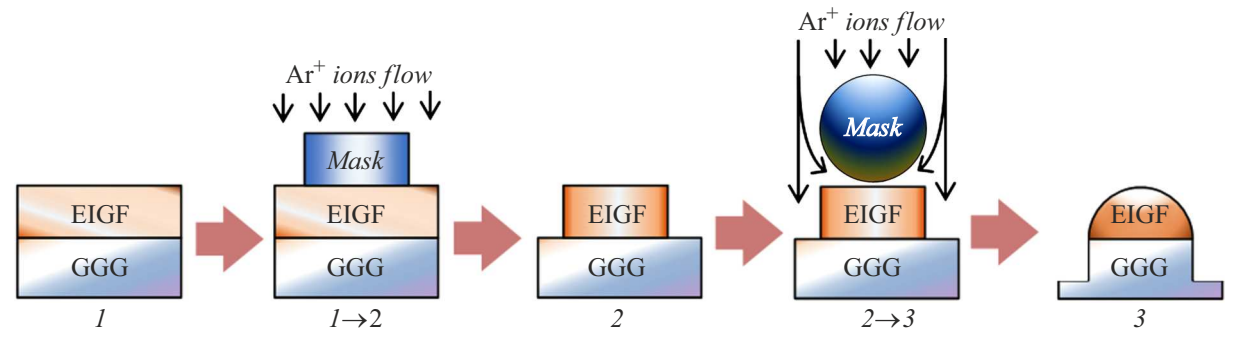


Figure 9. Stepwise scheme of formation of the elliptic profile of the iron garnet film in ion etching: I — the initial film; $I \rightarrow 2$ — etching with application of the disc-shaped mask R = 1.5 mm; 2 — the etching profile formed as a disc; $I \rightarrow 2$ — etching with application of the ball-shaped mask R = 1.5 mm; 3 — the final structure with the elliptic profile.

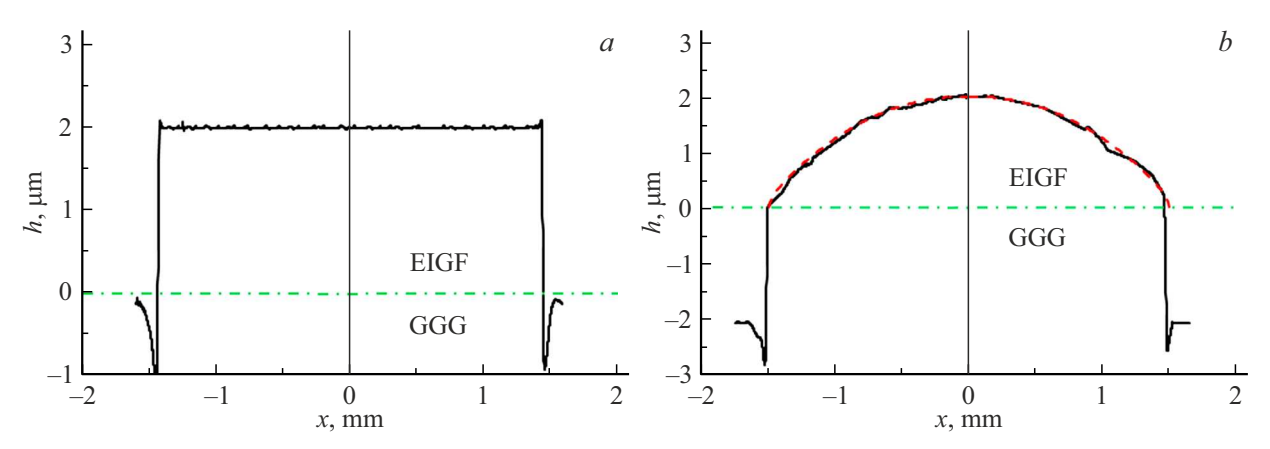


Figure 10. Cross-sectional profile of the formed surface using the disc-shaped mask (a) and subsequent application of the spherical mask (b). The dash-and-dot line marks a boundary between the EIGF film and the GGG substrate, the dashed line marks a model approximation of the etching smooth profile.

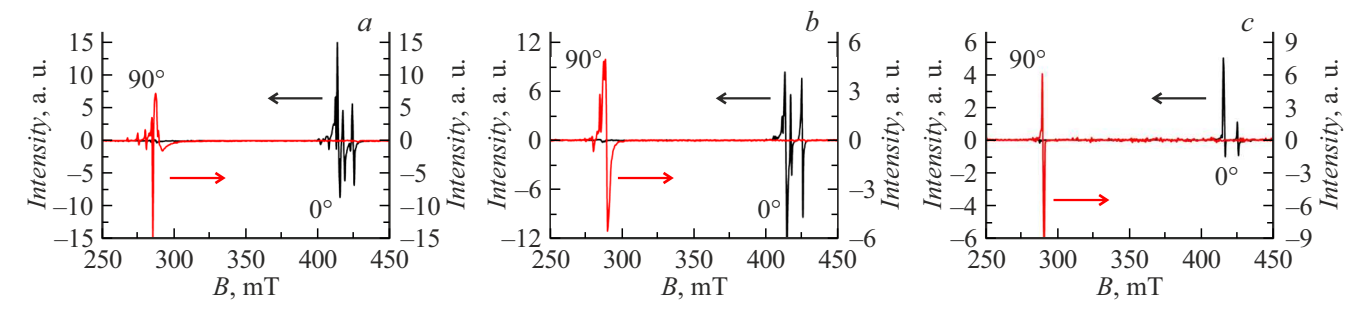


Figure 11. Resonance curves of FMR (the film $(YLa)_3(FeGaAl)_5O_{12}$, $h = 2 \mu m$) for parallel (90°) and perpendicular (0°) resonance: a — EIGF before treatment; b — the disc of the diameter of 3 mm (Fig. 9, a); c — the ellipse of the diameter of 3 mm (Fig. 9, b).

Fig. 10. It can be noted that after all the stages of etching there is significant reduction of intensity of and the number of the MSW modes, while the FMR resonance fields vary insignificantly.

Thus, with the perpendicular direction B, there are two signals: as the etching progresses, B_{res} varies from 414.1 to 415.4 mT and from 424.5 to 423.8 mT, respectively. With the parallel direction B_{res} varies from 287.2 to 290.5 mT. On the contrary, the value of the width of the FMR lines ΔB is reduced significantly. Thus, in case of the untreated film

sample (Fig. 11, a) ΔB in the perpendicular configuration is 2.0 and 1.3 mT, and in the parallel configuration it is 5.2 mT. After off-etching of the disc (Fig. 11, b) ΔB in the perpendicular configuration is reduced to 1.3 and 0.7 mT, and in the parallel configuration ΔB is 1.5 mT, respectively. After formation of the elliptic profile (Fig. 11, c), the width of the FMR line is reduced to 1.2 and 0.6 mT in the perpendicular configuration and to 1.3 mT in the parallel configuration, respectively. At the same time, it should be noted that after formation of the elliptic profile of the

sample the FMR spectra for the both configurations of *B* are completely free of noises caused by MSW and the edge defects, while the resonance lines are clear single peaks.

Thus, it is clear that the change of the spatial form of the film significantly affects the specific features of the resonance curves of FMR. Thus, the change of the EIGF form from the square to elliptic one results not only in reduction of the width of the resonance FMR line, but in elimination of the noises related to the edge defects and excitation of MSW.

Conclusion

The study presents the results of investigation of the influence of the various methods of post-growth treatment, namely, ion-plasma and acid etching of the surface of the epitaxial iron garnet films, on the change of the structural and magnetic resonance properties of these films. It is shown that when forming the various planar structures in etching through the mask both the methods demonstrate the similar results both in terms of the formed etching profile and of the properties of the produced structures as well.

The morphology of the EIGF surface in layer-by-layer etching by the various methods has been analyzed to show that the roughness parameters decrease as the etching progress, while the method of ion-plasma etching forms average smaller roughness of the film surface as compared to the method of acid etching.

When the planar geometry of the EIGF sample is changed both in the form (from the square to the disc) and the size (the disc diameter), the FMR spectrum exhibits the changes related to efficiency of excitation of the MSW modes as compared to the basic mode. It is shown that in etching through the disc-shaped mask the method of post-growth treatment insignificantly affects the form of the spectrum, as the form and the profile of the produced structures are almost the same both for ion and acid etching.

With layer-by-layer removal of the EIGF material, application of ion-plasma etching allows significantly reducing noise pollution of the resonance FMR signals as compared to using the acid method of etching, which is due to smaller parameters of surface roughness.

Formation of the elliptic etching profile of the iron garnet film when using the spherical masks allows significantly reducing the influence of the edge defects and completely eliminating MSW excitation, thereby resulting in excitation of the single clear FMR signals with the minimum width of the resonance lines.

Funding

The study was financially supported by a grant from the Russian Science Foundation (the project N_2 19-72-20154, https://rscf.ru/project/19-72-20154/).

Conflict of interest

The authors declare that they have no conflict of interest.

References

- [1] V.G. Vishnevskii, R.M. Mikherskii, S.V. Dubinko. ZhTF, 72 (2), 96 (2002) (in Russian).
- N. Lugovskoy, V. Berzhansky, D. Glechik, A. Prokopov.
 J. Phys.: Conf. Ser., 1124, 5 051063 (2018).
 DOI: 10.1088/1742-6596/1124/5/051063
- P.M. Vetoshko, N.A. Gusev, D.A. Chepurnova,
 E.V. Samoilova, I.I. Sera, I.M. Sera, A.K. Zvezdin,
 A.A. Korotaeva, V.I. Belotelov. Tech. Phys. Lett., 42 (8),
 860 (2016). DOI: 10.1134/S1063785016080289
- [4] S.L. Vysotskii, M.E. Seleznev, Yu.V. Nikulin, A.V. Kozhevnikov, G.M. Amakhanov, A.G. Temiryazev. FTT, 66 (7), 1057 (2024) (in Russian). DOI: 10.61011/FTT.2024.07.58373.34HH
- [5] A. Malozemov, Dzh. Slonzuski. Domennye stenki v materialakh s tsilindricheskimi magnitnymi domenami (Mir, M., 1982) (in Russian).
- [6] S.V. Levyi, Yu.S. Agalidi, V.G. Vishnevskii. Izvestiya vuzov. Radioelektronika, 41 (8), 74 (1998) (in Russian).
- [7] (U). Özgür, Y. Alivov, H. Morko, J. Mater. Sci.: Mater. Electron., 20 (9), 789 (2009).
 DOI: 10.1007/s10854-009-9923-2
- [8] R.M. Eguzhokova, A.I. Ivanova, E.M. Semenova. Fizikokhimicheskiye aspekty izucheniya klasterov, nanostruktur i nanomaterialov, 11, 123 (2019) (in Russian).
- [9] Yu.M. Bunkov. Phys. Usp., 53 (8), 848 (2010).DOI: 10.3367/UFNe.0180.201008m.0884
- [10] A. Ustinov, V. Kochemasov, E. Khas'yanova. Elektronika, 8 (00148), 86 (2015) (in Russian).
- [11] K.V. Bublikov, S.E. Sheshukova, E.N. Beginin, M. Tapajna, D. Gregusov, S.N. Krylov, A.I. Stognii, S.A. Korchagin, S.A. Nikitov, A.V. Sadovnikov. FTT, 65 (7), 1157 (2023) (in Russian). DOI: 10.21883/FTT.2023.07.55838.32H
- V.V. Tikhonov, V.A. Gubanov, A.V. Sadovnikov. Phys. Solid State, 63 (10), 1569 (2021).
 DOI: 10.1134/S1063783421090420
- [13] S.N. Polulyakh, V.N. Berzhanskii, E.Yu. Semuk, V.I. Belotelov, P.M. Vetoshko, V.V. Popov, A.N. Shaposhnikov, A.G. Shumilov, A.I. Chernov. ZhETF, 159 (2), 307 (2021) (in Russian). DOI: 10.31857/S0044451021020103
- [14] P.A. Popov, A.Y. Sharaevskaya, E.N. Beginin, A.V. Sadovnikov, A.I. Stognij, D.V. Kalyabin, S.A. Nikitov. J. Magn. Magn. Mater., 476, 423 (2019). DOI: 10.1016/j.jmmm.2018.12.008
- [15] A.I. Chernov, M.A. Kozhaev, D.O. Ignatyeva, E.N. Beginin, A.V. Sadovnikov, A.A. Voronov, D. Karki, M. Levy, V.I. Belotelov. Nano Lett., 20, 5259 (2020). DOI: 10.1021/acs.nanolett.0c01528
- [16] K.P. Belov. *Redkozemel'nye magnetiki i ikh primenenie* (Nauka, M., 1980) (in Russian).
- [17] V.V. Randoshkin, A.Ya. Chervonenkis. *Prikladnaya magnitooptika* (Energoatomizdat, M., 1990) (in Russian).
- [18] A.M. Balbashov. Elementy i ustroistva na tsilindricheskikh magnitnykh domenakh: spravochnik, pod red. N.N. Evtikhieva, B.N. Naumova (Radio i svyaz', M., 1987) (in Russian).
- [19] A. Eshenfel'der. Fizika i tehnika tsilindricheskikh magnitnykh domenov (Mir, M., 1983). [Per. s angl. A.H. Eschenfelder. Magnetic bubble technology (Springer, 1981)] (in Russian).
- [20] F.V. Lisovskii. Fizika tsilindrichekikh magnitnykh domenov (Sov. radio, M., 1979) (in Russian).
- [21] S.P. Zimin, I.I. Amirov, V.V. Naumov, M.S. Tivanov, L.S. Lyashenko, O.V. Korolik, E. Abramof, P.H.O. Rappl. FTT, 66 (8), 1408 (2024) (in Russian). DOI: 10.61011/FTT.2024.08.58608.131

- [22] M.V. Logunov, S.A. Nikitov, A.I. Stognii, S.S. Safonov, A.G. Temiryazev. Izv. RAN. Seriya fiz., 83 (7), 950 (2019) (in Russian). DOI: 10.1134/S0367676519070251
- [23] S.I. Yushchuk. ZhTF, **69** (12), 62 (1999) (in Russian).
- [24] V.I. Netsvetov, A.I. Kosse, V.V. Shchigolev, V.A. Khokhlov, Yu.V. Medvedev. Elektronnaya obrabotka materialov, 45 (4), 47 (2009) (in Russian).
- [25] N.I. Tsidaeva, A.T. Nakusov, S.A. Khaimanov, A.K. Khubaev, L.M. Kubalova, W. Wang. Tech. Phys., 65 (2), 276 (2020). https://doi.org/10.1134/S1063784220020243
- [26] W.A. Johnson, J.C. North, R. Wolfe. J. Appl. Phys., 44 (10), 4753 (1973). DOI: 10.1063/1.1662031
- [27] V.G. Kostishin, A.T. Morchenko, D.N. Chitanov, V.M. Trukhan. Materialy elektronnoi tekhniki, 3, 29 (2012) (in Russian).
- [28] A.A. Voronov, D.O. Ignatyeva, D. Karki, M.A. Kozhaev, M. Levy, V.I. Belotelov. Thirteenth International Congress on Artificial Materials for Novel Wave Phenomena, 447 (2019). DOI: 10.1109/MetaMaterials.2019.8900842
- [29] G.F. Ivanovskii, V.I. Petrov. *Ionno-plazmennaya obrabotka materialov* (Radio i svyaz', M., 1986) (in Russian).
- [30] A.G. Shumilov, A.A. Fedorenko, A.S. Nedviga, E.Yu. Semuk, I.A. Naukhatskii, V.N. Berzhanskii, A.N. Shaposhnikov, S.V. Tomilin. (Pat. RU 2 791 730 C1. Zayavl. 28.11.2022, opubl. 13.03.2023)
- [31] O.A. Tomilina, A.A. Syrov, S.V. Tomilin, V.N. Berzhanskii. Poverkhnost', 10, 29 (2022) (in Russian). DOI: 10.31857/S1028096022100156
- [32] P.M. Vetoshko, V.A. Skidanov, A.L. Stempkovskiy. Sensor Lett., 11 (1), 59 (2013). DOI: 10.1166/sl.2013.2768
- [33] S.A. Yur'ev, S.I. Yushchuk. Pribory i tekhnika eksperimenta, 6, 102 (2013) (in Russian). DOI: 10.7868/S0032816213050236
- [34] S.N. Ivanov, M.I. Bichurin, G.A. Semenov. Vestnik NovGU, 2 (73), 97 (2012) (in Russian).
- [35] V.A. Skidanov, P.M. Vetoshko. Procedia Enineering, 5, 989 (2010). DOI: 10.1016/j.proeng.2010.09.275
- [36] P.M. Vetoshko, A.K. Zvedin, V.A. Skidanov, I.I. Syvorotka, I.M. Syvorotka, V.I. Belotelov. Pis'ma v ZhTF, 41 (9), 103 (2015) (in Russian).

Translated by M.Shevelev